Proceedings of the International Conference on Heat Exchanger Fouling and Cleaning - 2024 (Peer-reviewed)
April 21–26, 2024, Lisbon, Portugal; Editors: H.U. Zettler and E.M. Ishiyama

EXPERIMENTAL STUDIES OF THE FLUSHING PROCESS OF CHOCOLATE FLUIDS IN A TEST FACILITY

***M. Heide[1], V. Liebmann[2], S. Kricke[1], F. Rüdiger[2], J.-P. Majschak[1] and H. Köhler[1]**
[1] Chair of Processing Machines/Processing Technology, Institute of Natural Materials Technology, TUD Dresden University of Technology, Germany, matti.heide@tu-dresden.de, +49 351 463-42382
[2] Chair of Fluid Mechanics, Institute of Fluid Mechanics, TUD Dresden University of Technology, 01062 Dresden, Germany

ABSTRACT

The chocolate processing industry offers a constantly growing variety of products. With a limited number of production lines in combination with complex components (e.g. shell-and-tube heat exchangers), product change is a critical step to ensure consumer safety and product quality. Product changes are achieved by displacing the product by a follow-up product. Within the scope of this work, the development of a test facility for the replication of industrial flushing processes is presented. The complexity of heat exchangers is reduced to a simplified double-pipe heat exchanger. A standardized methodology for operating and evaluating the experimental tests is presented. In combination with a short review of similar published investigations, this work contributes to the expansion of the experimental database on flushing processes. Parameter studies on the influence of the process temperature and order of flushing fluids are used to validate a numerical simulation model of the process.

INTRODUCTION

According to Classen and Hendrix, global competitions have led to a steady increase in the demand for different chocolate products in the past [1]. The demand ranges from dark chocolates with high cocoa content to chocolate containing milk solids, white chocolate, which contains only milk and no cocoa solids, or chocolate with exclusively vegan ingredients, to name just a few examples. This growing demand has required manufacturers to adapt their production processes. Expanding the manufacturing infrastructure to include dedicated lines for each chocolate involves significant costs and is usually not feasible, particularly for small to mid-sized businesses. For this reason, different chocolate products are manufactured in batches on the same line to achieve the diverse product range.

The process of changing the product between the production phases of the individual batches is known as the displacement process. In the context of chocolate manufacturing, it is referred to as flushing or purging. Here, this means that a chocolate is displaced from a pipeline by a follow-up chocolate or by intermediate products, e.g. cocoa butter. To ensure both product quality and consumer safety and to minimize the overall process cost, it is necessary to comprehend and optimize the flushing process.

The efficiency of the process depends heavily on the properties of the fluids, the process conditions, e.g., temperature or flow velocity, and lastly on the design of the production line and the pipeline components. Considering the variation in production line designs among manufacturers, a test facility was developed as a simplification of a production line containing the most commonly used components. The simplest form of heat exchangers, a double-pipe heat exchanger, was examined in this paper.

An outline of our paper is as follows. First, a short overview of current scientific work on flushing processes is provided. Subsequently, the materials and the experimental methods are described in detail. The paper then outlines a novel evaluation methodology for flushing experiments. Subsequently, a setup for a numerical simulation of the flushing process is described. Based on selected parameters, a comprehensive comparison between experimental and simulation results is presented. The paper concludes by summarizing findings and suggestions for future research.

DISPLACEMENT PROCESSES – A SHORT REVIEW

The research field of displacement processes is diverse and includes a variety of studies. In the following section, selected investigations will be divided into four main areas according to the main focus of the study: the displacing fluid has Newtonian behavior, the displacing fluid has non-Newtonian behavior, the density stability (density-stable/ density-unstable) of the fluids involved, and the orientation of the experimental setup (horizontal/ inclined).

Displacing fluid with Newtonian behavior

Subsequent authors investigated displacement processes in near horizontal pipelines using

ISBN: 978-0-9984188-3-4; Published online www.heatexchanger-fouling.com

Newtonian fluids as displacing fluids which where miscible with the displaced fluids.

Henningsson et al. [2] and Regner et al. [3] investigated the displacement of a non-Newtonian fluid (yogurt) by water in experiments and compared the results to a Computational Fluid Dynamics (CFD) simulation. Using electrical resistance tomography, they were able to visualize the distribution of the yoghurt over time in the experiments. The simulation revealed that an increase in yield stress reduces both yoghurt loss and the volume of mixing zone.

Moises et al. [4] used glycerol-water mixtures to displace a non-Newtonian fluid (Carbopol solution) and identified three distinct flow types, namely corrugated, wavy, and smooth, depending on the distribution of the residual layer along the pipe. It was found, that the type of flow regime depends on the Reynolds number ($Re = 0.2$ for wavy-corrugated and $Re = 1$ for smooth-wavy flow transitions).

Palabiyik et al. [5] investigated the use of water to displace a non-Newtonian fluid (toothpaste) from a horizontal pipe. Similar to Henningsson et al. [2], the investigated fluids were miscible and density-stable, the latter meaning that the density of the displacing fluid was lower than the displaced one [6]. They identified three flow regimes: core removal, film removal, and patch removal. They showed that the conditions during core removal significantly affect overall cleaning time [5]. Palabiyik et al. [7] extended these studies to other displaced fluids such as hand cream, apple sauce, yoghurt, and shower gel, and a dimensional analysis was used to explore the influence of different dimensionless parameter groups on the displacement process. It was stated that the ratio of yield stress to wall stress can be used to correlate the flushing behavior and flushing time of yield-stress fluids in pipes.

Taghavi et al. [8] investigated the displacement process of miscible, density-unstable Newtonian fluid pairings (Glycerol-water solutions). They investigated different flow velocities and observed the development of different displacement fronts. They identified five to six flow regimes and characterized them as either inertial or viscous flow regimes. Taghavi et al. [9] extended these investigations to non-Newtonian displaced fluids (Carbopol solutions). They observed two flow regimes: center-type and slump-type. The transition between both regimes appear to be mainly dependent on a critical threshold in the ratio of Reynolds and Froude number.

Displacing fluid with non-Newtonian behavior

Taghavi et al. [10] investigated the displacement processes in horizontal pipes involving both Newtonian fluids (Glycerol-water mixtures enriched with or without NaCl) and non-Newtonian fluids (Xanthan). They tested three configurations: (a) shear-thinning fluid displacing Newtonian fluid, (b) Newtonian fluid displacing shear-thinning fluid, and (c) shear-thinning fluid displacing shear-thinning fluid. The study focused on examining the impact of shear-thinning fluids as well as varying viscosity ratios on the displacement process. They determined the displacement efficiency based on the ratio of the mean flow velocity to the front velocity. Their studies confirmed that the displacement efficiency decreases when the ratio of the viscosity of displaced to viscosity of displacing fluid increases.

In contrast, Gabard and Hulin [13] focused on the iso-dense displacement process in vertical pipes. They investigated three different types of fluid pairs with different rheology of displacing fluid and displaced fluid, respectively: (a) Newtonian – Newtonian fluids, (b) shear-thinning non-Newtonian – Newtonian fluids, and (c) non-Newtonian fluid with yield stress – Newtonian fluid.

Wiklund et al. [12] investigated various model and industrial fluids, such as yoghurt, xanthan, and sunflower oil, with different rheological behaviors and miscibility. They used a horizontal pipe system with an integrated measuring system to conduct the velocity profiles of different fluid pairs. In experiments with Newtonian – non-Newtonian fluid pairs, irregular velocity profiles were observed when the displaced fluid had a lower viscosity than the displacing fluid (refer to as viscous fingering). This occurred with both miscible and immiscible fluid pairs.

Orientation of the experimental setup

Subsequent authors [6, 16 - 18] investigated displacement processes in inclined or vertical pipelines in order to determine the influence of gravity.

Alba et al. [6] investigated the density-stable displacement flow of two miscible iso-viscous Newtonian fluids (water and NaCl-enriched water). They stated that the length of the interface along the pipe (called stretch length) decreases with inclination from near horizontal to vertical and increases for higher fluid viscosity.

Hasnain et al. [16] analyzed the displacement flow of two immiscible iso-viscous Newtonian fluids in inclined pipes (Range $5°$ - $90°$) They identified three main regimes, which are dependent on the Reynolds number and a function of the inclination. Low Reynolds numbers and inclinations are classified as “viscous”, higher inclinations at low Reynolds numbers ($Re < 750$) are classified as “transitionary” and the remaining regime as “dispersed”.

Alba et al. [17] extended their studies to inclined pipes with displacement experiments of a Newtonian fluid displacing a yield-stress fluid (Carbopol). Similar to Taghavi et al. [9], they observed both flow regimes: center and slump-type. They discovered that the transition between the two

ISBN: 978-0-9984188-3-4; Published online www.heatexchanger-fouling.com

regimes occurs in the range between $600 < Re/Fr < 800$ and that the angle of inclination therefore does not directly determine the flow regime. In Addition to the named flow types they observed another type: turbulent/ mixed-type, which appears when the flow is turbulent

Alba and Frigaard [18] expanded these investigations and focused on the development of the displacing front. They proved that the influence of inclination angle is not significant for the front velocities. They showed that the front velocity is always lower for center-type flows than for slump-type flows.

Density stability

Alba et al. [6] also investigated the density influence and revealed that density-stable configurations led to highly efficient displacements, with the interface moving steadily at the mean velocity.

Zare and Frigaard [14] supplemented the comprehensive analysis of the complex effects of fluid density ratios on the displacement process by applying Newtonian fluids as displacing and non-Newtonian fluids as displaced fluids, and by considering density-unstable configurations. Similar to Taghavi et al [9], they explored two major flow regimes, center-type and slump-type, which were determined in their studies by the density difference between the fluids. Zare et al. [15] completed the investigation by studying the flushing process of density-stable configurations using Bingham fluids as displaced and Newtonian fluids as flushing fluids.

Experimental methods of the studies

Different experimental methods were used to investigate the flushing process. Palabiyik et al. [5, 7] used a weighing analysis. In discrete time intervals, they removed the measuring pipe, carefully emptied it and weighed the remaining displaced fluid mass. The measuring pipe was then reinserted and the experiment continued. Henningsson et al. [2] and Regner et al. [3] used an electrical resistance tomography to measure the fluid distribution with a total monitoring frequency of 6.5 Hz. They used image reconstruction methods to present local and time-resolved fractions of different fluids in the pipe. Alba et al. [6] used a simple optical measurement method. They placed two digital high-speed cameras with 4096 grayscale levels in front of the measuring pipe and examined the flushing process with different colored liquids. Taghavi et al. and Moises et al. [4, 8-11] used the same optical method but supplemented this with an ultrasonic Doppler velocimeter (UDV) and additional particles to measure the present velocity profile of the fluids. Wiklund et al. [12] used a similar method. They combined an Ultrasound Doppler Velocity Profiling (UVP) and pressure difference (PD) technique to monitor the development of the velocity profile, mixing zones, and rheological changes in real-time. Lastly, Gabard and Hulin [13] utilized four pairs of acoustical transducers and a camera system to monitor the fluctuations of the fluid concentration.

Research gap

In the literature presented, the displacement process, also referred to as the flushing process, is introduced and a selection of factors influencing the process are highlighted. The majority of the research considers the displacement process of at least one fluid with non-Newtonian behavior. In the chocolate flushing process, however, both fluids have non-Newtonian behavior.

Within the presented state of research, there are only two experimental investigations addressing this fluid pairing: (non-Newtonian fluid displacing another non-Newtonian fluid)), one in horizontal [12] and one in vertical [13] pipe flows. Wiklund et al. [12] investigated the applicability of an in-line rheometer to monitor the flushing process of various foods like yoghurt and sunflower oil. They did investigate non-Newtonian fluids but mainly focused on fluids with lower apparent viscosities (< 1100 mPas). In addition, an inline measurement method was used, but the actual distribution in the pipe was not visually verified in the publication.

Furthermore, different experimental methods are mentioned in the literature to describe the distribution of the fluid after or during the displacement process in the pipe. Due to the opaque and generally similar properties (e.g. density) of the chocolates, most of the methods are not suitable for describing the distribution inside the pipe. The following work is intended to contribute to the aforementioned investigations, to extend them to the flushing process of chocolate in horizontal pipes and to provide a direct visualization of the distribution of fluids after the process using a novel experimental method.

MATERIALS AND METHODS

Materials

Two chocolate fluids were considered as displacing and displaced fluids: a white chocolate with low apparent dynamic viscosity and a dark chocolate with comparatively higher apparent dynamic viscosity than the white chocolate at all shear rates. In its melted state at temperatures above 35 °C, chocolate is a suspension of sugar particles and cocoa particles in a continuous liquid fat phase [19]. According to Kumbár et al. [20], the flow behavior is non-Newtonian. As described in Liebmann et al. [22] the rheological properties were determined using a HAAKE Mars 60 rheometer (Thermo Fisher Scientific Inc., USA) in double determination using a CC25 DIN/Ti 02180077 cylinder geometry in accordance with method 46 of the International Confectionary Association (ICA) [23]. The non-Newtonian behavior of the chocolate

ISBN: 978-0-9984188-3-4; Published online www.heatexchanger-fouling.com

fluid was then described through the application of the Windhab model as shown in Eq. (1) [24] by fitting the rheological data.

$$\tau = \tau_0 + \eta_\infty \dot{\gamma} + (\tau_1 - \tau_0) \cdot \left\{1 - \exp\left(-\frac{\dot{\gamma}}{\dot{\gamma}^*}\right)\right\} \quad (1)$$

Where τ_0 is the yield stress, $\dot{\gamma}$ the shear rate, η_∞ the dynamic equilibrium viscosity, τ_1 the extrapolated shear rate, and $\dot{\gamma}^*$ is the reference shear rate. Table 1 presents the resulting model constants for the three temperature levels (40 °C, 45 °C and 52 °C), which were investigated experimentally and numerically.

Table 1. Model parameters of selected chocolates at different temperatures describing the rheological behavior according to the Windhab model

	ϑ in °C	τ_0 in Pa	τ_1 in Pa	$\dot{\gamma}^*$ in 1/s	η_∞ in Pa s	R^2
white	40	8.59	12.73	6.87	1.35	0.9987
	45	8.42	12.16	6.56	1.14	0.9989
	52	8.23	11.81	6.85	0.89	0.9989
dark	40	21.73	40.77	8.02	2.88	0.9981
	45	20.29	38.72	8.94	2.42	0.9987
	52	18.88	33.61	9.35	1.93	0.9989

As reported in Liebmann et al. [21], the densities of both fluids were determined experimentally using a Coriolis flow meter H100S (Emerson Process Management GmbH & Co. OHG, USA). Both showed constant values across the three temperature levels. For further investigations, the density was therefore set at 1200 kg/m^3 for white chocolate and 1260 kg/m^3 for dark chocolate, resulting in a density ratio of almost unity.

Design of the test facility

Figure 1 shows the schematic structure of the test facility. It consists of two separate main circuits for chocolate flow, each with a heated stirring tank type EBB90RWA (93l capacity, Inox Behälter GmbH, Germany) and a rotary lobe pump type DK 500 ($n_{max} = 49\,min^{-1}$; Rinsch GmbH, Germany), as well as a measuring section, a disposal tank and a return line.

The heated and pneumatic three-way entry and exit valves type 3F25-H (Rinsch GmbH, Germany) integrated in the test facility before and after the measuring section enable the displaced fluid and the flushing fluid (referred to as displacing fluid) to be varied for the experiments. It is also possible to change the return line to the tank depending on the displaced fluid selected in the experiment.

The two circuits, along with the return line, enable the chocolate fluids to be circulated and evenly tempered prior to the experiment. In addition, a pigging system is integrated in the test facility, which was used for emptying the measuring section in between the experiments only.

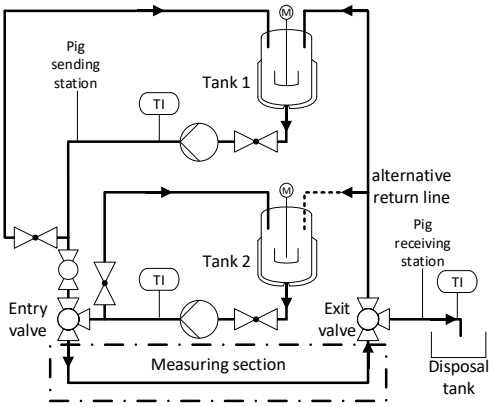

Fig 1. Schematic structure of the main piping system.

The entire test facility contains two separate indirect heating systems to ensure that the chocolate remains at a constant temperature during the experiments: (i) heating of the jacketed pipes with water as heating medium, and (ii) electrical trace heating. The latter was only used for selected complex components (e.g. T-pieces, valves) where the former method could not be applied. The temperature of the chocolate was monitored at selected positions using invasive temperature sensors. For the measuring section, solely non-invasive sensors were used in order to avoid influencing the flushing process.

The horizontal measuring section is shown in Figure 2 and contains three identical measuring section segments (referred to as segments) at distances of approximately one meter in order to be able to investigate the flushing progress at different stages simultaneously during one experiment. A coriolis sensor was installed solely during flow and density measurements; a straight pipe subsequently replaced it during the flushing experiments. With the exception of the entry valve and a pipe bend at a distance of approx. 0.3 m upstream from segment one, the measuring section consists only of straight pipe components. The whole measuring section has an internal diameter of 26 mm.

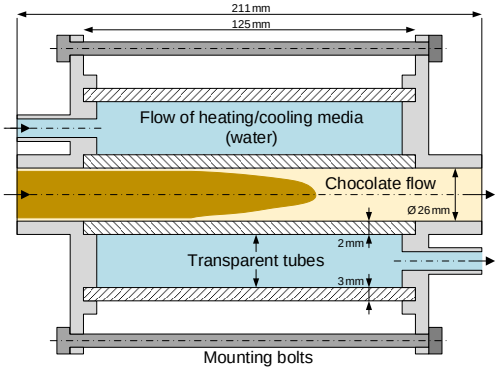

Fig 2. Schematic layout of the measuring section segment (simplified double pipe heat exchanger).

ISBN: 978-0-9984188-3-4; Published online www.heatexchanger-fouling.com

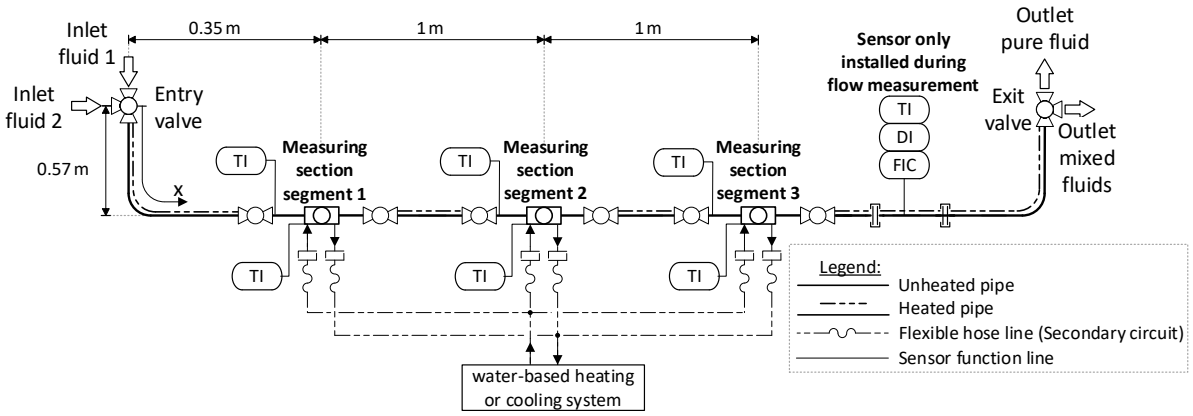

Fig 3. Schematic representation of the measuring section with sensors and the positioning of the three measuring section segments

A circulation cooler type UC 4 (Lauda Dr. R. Wobser GmbH & Co. KG, Germany) integrated into the test facility enables cooling of the segments using specific valve configurations. Figure 3 illustrates the schematic structure of a segment, along with the primary and secondary flows entering and exiting the segment. The segments represent simplified double-pipe heat exchangers that can be disassembled, are temperature regulated, and are additionally transparent. The latter allows for future utilization of visual measurement methods (e.g. color sensors).

Flow measurements

The correlation between pump setpoint speed n_{sp} to maximum pump speed $n_{\max}$ and actual flow rates was determined through reference flow measurements at different temperatures using a coriolis flow meter. Based on the actual flow rates, the mean bulk velocities were calculated for both chocolate fluids in fully filled pipes.

Table 2. Flow rates and flow velocities for selected chocolate fluids and temperatures

	ϑ_{sp} in °C	ϑ_{exp} in °C	$\frac{n_{sp}}{n_{max}}$ in %	$\dot{m}$ in kg/h	u_b in cm/s	u_{max} in cm/s
white	40	42.7	10	61	2.7	4.2
		42.9	20	125	5.5	9.2
	45	46.3	20	123	5.4	8.9
	52	52.7	20	119	5.2	8.3
dark	40	40.8	10	61	2.5	3.9
		41.2	20	126	5.2	8.7
	45	44.5	20	126	5.2	8.6
	52	50.6	20	126	5.2	8.4

Using the average bulk velocities and rheological parameters, the individual velocity profiles [25] were determined and the corresponding values for the maximum flow velocities were derived (see Table 2). The Reynolds number calculated based on the equilibrium viscosity is on the order of unity for all cases. The flow rates differ only slightly depending on the fluid, and the influence of temperature is higher for white chocolate than for dark chocolate.

Experimental procedure

A flushing experiment includes the steps:

I. The chocolates are melted in the tanks (melting time t_m~4 h, melt temperature ϑ_m~40 °C).
II. Both chocolate fluids are pumped through the corresponding circuits, the pipeline is vented and heated to the set temperature of the respective experiment.
III. The first chocolate is pumped through the measuring section and through the return line back into the corresponding tank for at least 15 minutes. The section is completely filled with the chocolate and all components show the same temperature.
IV. The pump of the first fluid is stopped, the pump of the flushing fluid is started and the entry and exit valves are switched simultaneously.
V. After reaching the flushing time t_{fl}, the pump is turned off and the streamwise direction flow of chocolate is prevented by closing the valves before and after each segment.
VI. The segments are then cooled for 20 minutes, removed from the measuring section and the evaluation method is applied
VII. Finally, the segments are replaced by simple pipes and the measuring section is pigged. All segments parts are then cleaned manually and the segments are reassembled.

Evaluation method

Following the flushing experiment, the individual measuring section segments, see Fig 2, were indirectly cooled with water at a temperature of $\vartheta_{co} = 9$ °C for a cooling time of $t_{co} = 20$ min using the circulation cooler. The cooling time was

ISBN: 978-0-9984188-3-4; Published online www.heatexchanger-fouling.com

determined in preliminary tests. A gravity-induced movement of the chocolates at rest did not occur within that time due to the almost identical density values and rapid solidification.

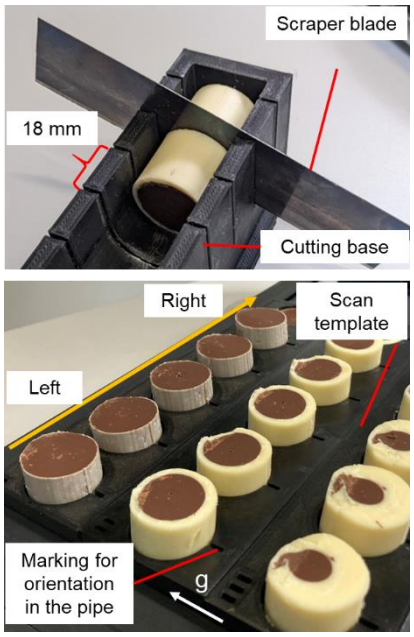

Fig 4. a) Cutting procedure and b) preparation for the digitalization of cross-sections using scan templates. Left and right indicate the position in the removed segment. The marking in the scan template shows the former alignment of the cross-section in the segment (marking at the highest point)

After cooling, the segments were removed from the measuring section, disassembled and the individual solid chocolate cylinders were pressed out of the transparent pipe with a piston and placed in a cutting base (see Figure 4a). Using a scraper blade and predefined blade guidance in the base, six cross-sections per chocolate cylinder were produced afterwards.

The cross-sections were positioned in a scan template according to the marks for orientation in the pipe and the position of the cross-sections in the measuring section segment for reproducible alignment as shown in Figure 4b. A flatbed scanner Lide 400 (Canon, Japan) with a resolution of 5.3 µm in the selected area was used to digitalize the cross-sections. Finally, the images were analyzed using a custom script in Matlab. The method is shown in Figure 5 and is described subsequently.

At the beginning, the image of one experiment is divided into individual images by defining regions of interest (ROIs) for each cross-section. Figure 5 shows examples of individual cross-sections for each segment. The individual images were then converted into grayscale images, the outer border of the presented cross section was automatically detected using the "imfindCircles" function (Figure 5b), and the region beyond the cross section border was masked. Subsequently, the image was binarized using a threshold value.

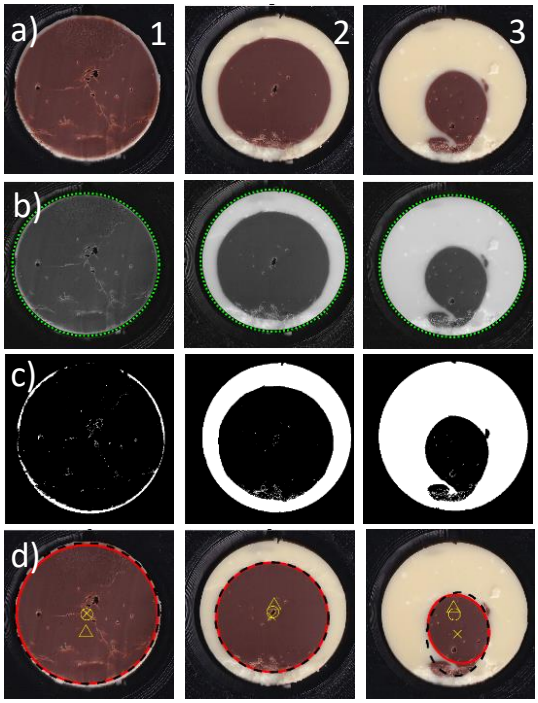

Fig 5. Image processing and evaluation method (e.g. $\vartheta = 40\,°\mathrm{C}$, $n_{sp}/n_{max} = 20\,\%$, $\mathrm{t} = 40\,\mathrm{s}$). 1 – 3 representing segments. a) Original image, b) Gray scale image with detection of outer contour, c) Binarized image with masking of outer contour and improvement of contours and surfaces d) Final results with contour detection (manual: solid line, automatic: dotted line) and center of area (flushing fluid: x, displaced fluid: Δ, center point: ○)

In addition, smaller gaps were automatically filled and the contours closed (Figure 5c). The target values were determined in the final step (Figure 5d). These encompass (i) the surface area of the individual chocolate fluids (displaced and flushing fluid) within the cross section (A_d, A_f), (ii) the fraction of the chocolate fluids' area in relation to the total area of the cross section (AR_d, AR_f) and (iii) the centroid of the areas. The following three methods were used to determine the target values: (A) sum of the white and black pixels in the ROI of the image, (B) manual fit of an ellipse, and (C) automatic fit of an ellipse. The measured values of the six cross-sections obtained from each segment were averaged, as the streamwise distance between them was not significant compared to the total distance of the measuring section.

Numerical setup

The numerical simulations were conducted using the multiphaseInterFoam solver from OpenFOAM v7. The continuity and momentum equations are solved. Additionally, a transport equation for a scalar α is solved using the volume of

ISBN: 978-0-9984188-3-4; Published online www.heatexchanger-fouling.com

fluid method. The value of α in each cell indicates the fraction filled with the flushing fluid.

The computational domain consists of a part of the measuring section shown in Figure 2. The inlet of the numerical domain corresponds to the outlet of the entry valve. In flow direction, it contains a piece of straight section, a 90 ° elbow bend and a second straight section. The end of the second straight section corresponds to the outlet of the first measuring section segment.

The computational domain is sketched in Figure 6 along with the numerical grid, which is linearly extruded along the pipe axis. The values for the pipe radius $R = 0.013\,\mathrm{m}$, the length of the first straight section $L_z = 0.48\,\mathrm{m}$, the pipe bend radius $r_{\mathrm{pb}} = 0.07\,\mathrm{m}$ and the second straight section $L_x = 0.4\,\mathrm{m}$ correspond to the values of the parts used in the measuring section of the test facility. This results in a total number of approximately 1.6 million cells.

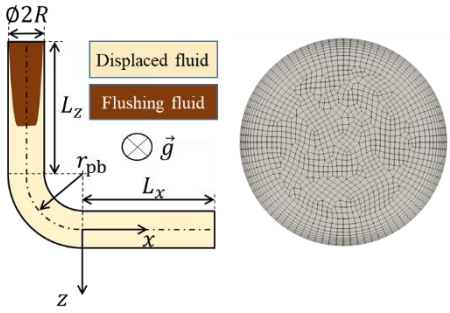

Fig. 6. Sketch of the computational domain (left) and the grid for one cross section (right) [21]

Eight simulations were conducted. For each, the flushing fluid velocity and temperature of both fluids correspond to one row in Table 2. At the inlet, the flushing fluid enters the domain, i.e., $\alpha = 1$. The velocity distribution at the inlet corresponds to the analytical solution of developed flow of the flushing fluid in a pipe, taken from the literature [25]. For each simulation, the resulting bulk velocity u_{b} corresponds to the experimental value shown in Table 2. The remaining pipe is initially filled with the displaced fluid at rest. As described in [21, 22] the rheological properties are modeled using the Windhab model, which has been implemented in OpenFOAM. To limit the viscosity, a regularization parameter ν_{max} was added.

Design of experiments

In the following, two parameter studies were conducted. In study one the process temperature was varied on three levels (40 °C, 45 °C and 52 °C) and the individual experiments were considered isothermal. A dark chocolate was used to displace white chocolate (also referred to as WCDC) at a constant pump rate of $n_{\mathrm{sp}}/n_{\mathrm{max}} = 20\,\%$ and a constant flushing time $\mathrm{t_{fl}} = 40\,\mathrm{s}$.

In study two, the displaced and the flushing fluid were varied for two selected flow rates (Case I: $\frac{n_{\mathrm{sp}}}{n_{\mathrm{max}}} = 10\,\%$ and Case II: $\frac{n_{\mathrm{sp}}}{n_{\mathrm{max}}} = 20\,\%$) at constant temperatures. Two configurations were examined: A white chocolate was used as flushing fluid and a dark chocolate as displaced fluid (WCDC) and a dark chocolate was used to displace a white chocolate (DCWC). For a lower pump rate the flushing time was set to $\mathrm{t_{fl}} = 80\,\mathrm{s}$. All experiments were done at least in triplicate, with a total of 18 experiments.

RESULTS AND DISCUSSION

A dimensionless presentation of the target values, as proposed in [21], was used to facilitate comparing the flushing progress in different segments despite their varied position in the measuring section. Equations (2) and (3) show the corresponding dimensionless variables. It also facilitated the comparison with the flushing simulation, which included only the first measuring section segment in its computation domain.

$$\hat{t} = \frac{u_{\mathrm{max}} \cdot t_{\mathrm{fl}}}{x} \qquad (2)$$

$$1 - \frac{r_{\mathrm{c}}}{R} = 1 - \sqrt{AR_{\mathrm{f}}} \qquad (3)$$

The characteristic sequence of the flushing process is shown in Figure 7 using the simulation curve. An increase in the value $\hat{t}$ reflects the progression of the flushing process in the section under consideration. As $\hat{t}$ progresses, the proportion of the displaced fluid within the section decreases. The regions known from the literature [5, 21, 22] can be observed. In phase $0 < \hat{t} < 1$ the flushing fluid has not yet reached the area under consideration (e.g. segment one with $x = 0.92$ m). Therefore, no change in fluids concentration occurs in this phase. Beginning with $\hat{t} = 1$, the core removal phase takes place and the majority of the first fluid is flushed out of the segment. This is followed by the phase of layer removal in a smooth transition.

To compare experimental and numerical results, the experimental data from the cross sectional images have to be converted using an area-equivalent circular shape with a radius r_{c}. The percentage of flushing fluid in the examined area is represented by the ratio of the cleaned radius r_{c} to the inner pipe radius R and derived using equation (3).

Parameter study 1: Influence of process temperature

Figure 7a presents the experiments and simulation for the configuration WCDC, the process temperature 40 °C and 20 % pump power. Methods A, B and C (c.f. section evaluation methodology) were used to determine the target value AR_{f}. Figure 7b shows the comparison of the individual methods against each other and the deviations from the simulation data. The standard deviation was

ISBN: 978-0-9984188-3-4; Published online www.heatexchanger-fouling.com

determined and averaged for six cross sections of a segment as the data basis for the respective method. This approach was applied three times. Segments 1 and 2 exhibited no significant differences among methods A to C. Conversely, in segment 3, slight deviations between methods were observed, but these were not significant compared to the general measurement inaccuracies.

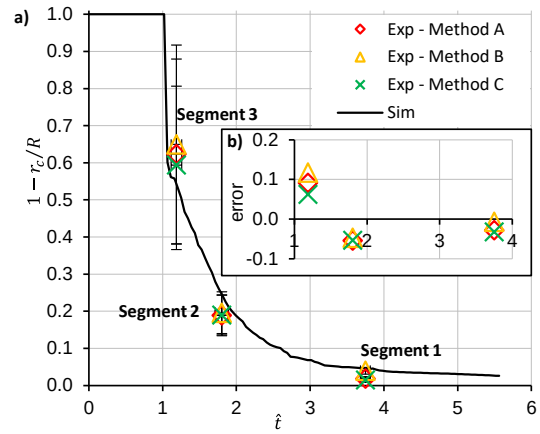

Fig. 7 a) Cleaned radius vs. dimensionless time, b) error between experiment and simulation with the three different methods for WCDC with $\vartheta = 40\,°C$, $n_{sp}/n_{max} = 20\,\%$, $t_{fl} = 40\,s$

Upon considering the overall measurement dataset, no clear tendency was recognizable. To reduce the overall shown data only the target values according to method B will therefore be presented in the following diagrams.

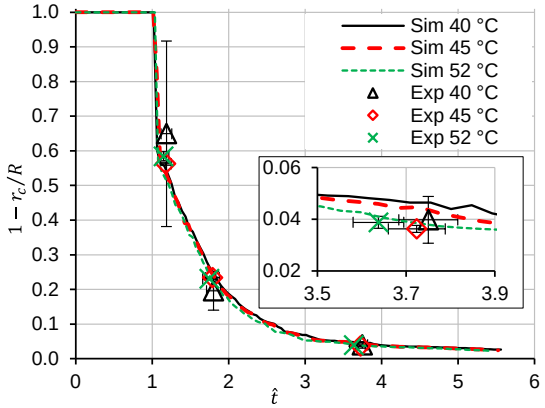

Fig. 8. Experiment vs. Simulation (WCDC): Temperature variation with $n_{\mathrm{sp}}/n_{\mathrm{max}} = 20\,\%$, $\mathrm{t_{fl}} = 40\,s$. Inset figure shows the deviation between experiments and simulation.

Figure 8 presents the numerical and experimental results of the first parameter study. It is evident, that the experimental results barely deviate from each other and from the numerical results at different temperatures. This is also consistent with the simulation studies from [21], where the uniform heating of both fluids also leads to similar changes in viscosity, and the viscosity ratio therefore remains the same. It can also be seen that the deviations in the area fractions and r_c are greater the closer the flushing front is to the segment under consideration ($\hat{t} \to 1$), due to a higher sensitivity. The error of the dimensionless time depends on the measurement inaccuracies of the maximum flow velocity Δu_{max} (approx. ± 3 %), the pipe distance Δx (approx. ± 0.005 m), and the flushing time Δt_{fl} (approx. ± 2 s).

Parameter study 2: Influence of fluid properties

In Figure 9 the Case I of experimental and simulation results from the second parameter study are presented. Here the configuration DCWC demonstrates a more effective removal at the beginning of the process ($1 < \hat{t} < \sim 1{,}4$) compared to the alternative configuration. This is due to the lower viscosity of the white chocolate and the resulting higher flow velocity. The cross-sectional images show anomalies in the distributions of the DCWC configuration, particularly in the area of the third segment, which explain the strong measurement deviations in this area.

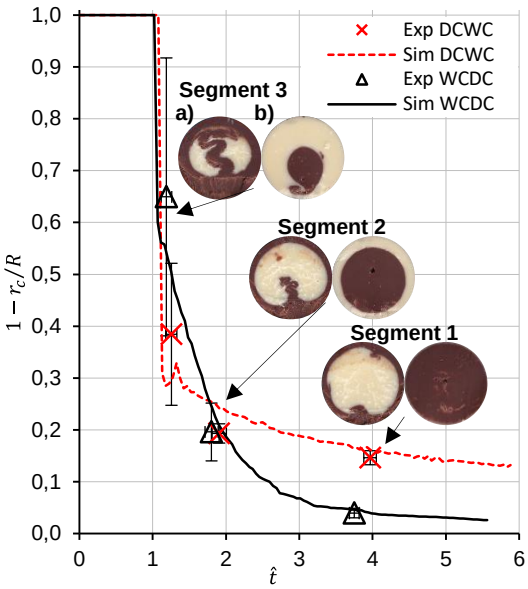

Fig. 9. Experiment vs. Simulation: Variation of fluids (Case I). (a) DCWC and (b) WCDC for $\vartheta = 40\,°C$, $n_{\mathrm{sp}}/n_{\mathrm{max}} = 20\,\%$, $\mathrm{t_{fl}} = 40\,s$.

This could be due to the initial contact of the fluids in the entry valve or also to the abrupt stop of the flow at the end of the experiment. The identification of the cause is part of future investigations. At around $\hat{t} \approx 1{,}4$, a brief decrease can be seen in the simulation of the DCWC configuration. It is assumed, that the flushing fluid constricts upstream of the front and thus the contact or cleaning radius decreases slightly when this constriction passes through the measuring section. For higher dimensionless times, the dark chocolate

ISBN: 978-0-9984188-3-4; Published online www.heatexchanger-fouling.com

with higher viscosity flushes the white chocolate from the pipe much faster than in the other configuration. This was also reported previously by [10, 11].

Figure 10 displays the experimental and numerical results for Case II of the second study, conducted with a lower flow rate. Compared to Figure 9, the same characteristic curves appear. With regard to extended simulation data, a lower flow rate leads to minimally higher cleaned radii, which means that using the same amount of flushing fluid leads to higher cleaned radii in the case of lower flow rates. In addition, the cross-sectional images show a similar distribution to the results from the first part of the study.

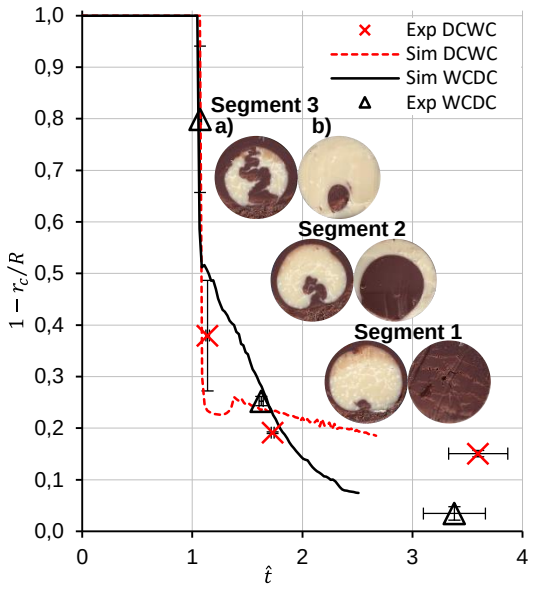

Fig. 10. Experiment vs. Simulation: Variation of fluid (Case II). (a) DCWC and (b) WCDC for $\vartheta = 40\,°C$, $n_{sp}/n_{max} = 10\,\%$, $t_{fl} = 80\,s$.

However, this also increases the required flushing time. Depending on the system operator, it must therefore be determined whether the flushing fluid or flushing time should be minimized.

The assumption that the flushing front forms a circular shape in the cross-sections was not fulfilled in tests with white chocolate as the flushing fluid, for low dimensionless times (see Figure 9 and Figure 10). Despite this deviation from the initial assumption, an overall high level of agreement was observed between the experimental and simulation results.

CONCLUSION

In summary, this research contributes to the understanding of the flushing process of two non-Newtonian fluids in the food sector, using the example of chocolate processing. We developed a test facility and a novel methodology to quantify the influence of the selected fluids and process parameters on the flushing process in horizontal and straight pipelines. Three methods for determining the fraction of flushing fluid in the cross section image were investigated and compared. The methods showed only slight differences in the results. For future investigations, we preferably will use the automated method A and for selected cross section images additionally the manual method B to further cross validate method A. A successful replication of the industrial process of a simplified heat exchanger was achieved by developing a measuring section segment and implementing it in the test facility. In addition, numerical simulations were conducted, the results were compared and validated using equivalent flushing experiments.

The results revealed the occurrence of the regimes known from [5] in every configuration examined, whereby only core removal and film or layer removal were observable. Patch removal was not detected. This could be either due to the resolution limitations of the measurement method or its absence in the considered configuration due to too short flushing times. It was demonstrated, that the influence of the process temperature on the flushing process is not significant for the isothermal case.

Consistent with the observations from Taghavi et al. [10] and despite the differences in the fluids used, the viscosity ratio was found to have a strong influence on the flushing process. We were able to confirm that when a fluid with higher viscosity was used to displace a fluid with lower viscosity, it resulted in higher efficiency compared to displacing a fluid with higher viscosity using a low viscosity fluid.

Although a good agreement of the experimental data with the simulations is achieved, it is important to consider the limitations of the study. First, the experimental investigations using the present test facility currently can only be realized with a limited selection of fluids (depending on the yield stress and the apparent viscosity) due to the limited pumping capacity of the pumps. Second, the developed evaluation method requires that the investigated fluids differ in color. Third, the method is currently only applicable for simple double-tube heat exchangers and requires adaptation for other complex components. However, slight modifications of the test facility and its components allow the investigation of other pipeline components and fluids (e.g. oil, cosmetic) in the future.

Looking ahead, in line with the statement made in [5] future research should investigate the effects of more complicated components (such as valves, T-pieces, extensions and reductions, shell-and-tube heat exchangers) on the flushing process. In combination with the validated simulations, it would be possible to model individual production lines and optimize the flushing process using the knowledge of the fluid properties.

ISBN: 978-0-9984188-3-4; Published online www.heatexchanger-fouling.com

ACKNOWLEDGMENTS

The authors gratefully acknowledge the support of Leslie Angela Knipping, Chair of Processing Machines/Processing Technologies, by supporting the measurements. This research project is supported by the Industrievereinigung für Lebensmitteltechnologie und Verpackung e.V. (IVLV), the Arbeitsgemeinschaft industrieller Forschungsvereinigungen, Otto von Guericke‘ e.V. (AiF) and the Federal Ministry of Economic Affairs and Climate Action (AiF Project IGF 20672 BR).

NOMENCLATURE

Latin symbols

A	Surface area, m²
AR	Surface area ratio, dimensionless
n	Pump speed, min^{-1}
r	Radius, m
R	Pipe radius, m
t	Time, s
$\hat{t}$	Dimensionless time, dimensionless
u	Flow velocity, m s^{-1}
x	Distance to the entry valve, m

Greek symbols

α	Percentage of flushing fluid in the considered total volume, dimensionless
$\dot{\gamma}$	Shear rate, s^{-1}
$\dot{\gamma}^*$	Windhab model parameter, 1/s
η_∞	Windhab model parameter, Pa s
ϑ	Temperature, °C
ρ	Density, kg m^{-3}
τ	Stress, Pa
τ_0	Yield stress, Pa
τ_1	Windhab model parameter, Pa

Subscript

b	bulk
c	cleaning/ contact
co	cooling
exp	experimental
f	flushing fluid
fl	flush
m	melt
max	maximum
d	displaced fluid
pb	pipe bend
sp	set point

REFERENCES

[1] Claassen, G. D. H., and Hendrix, Eligius M. T., On Modelling Approaches for Planning and Scheduling in Food Processing Industry. In Lecture Notes in Computer Science (pp. 47–59). Springer International Publishing, 2014.

[2] Henningsson, M., Regner, M., Östergren, K., Tragårdh, C., and Dejmek, P., CFD simulation and ERT visualization of the displacement of yoghurt by water on an industrial scale. *Journal of Food Engineering*, 80(1), 166–175, 2007.

[3] Regner, M., Henningsson, M., Wiklund, J., Östergren, K., and Trägårdh, C., Predicting the displacement of yoghurt by water in a pipe using CFD. *Chemical Engineering & Technology*, 30(7), 844–853, 2007.

[4] Moisés, G. V. L., Naccache, M. F., Alba, K., & Frigaard, I. A., Isodense displacement flow of viscoplastic fluids along a pipe. *Journal of Non-Newtonian Fluid Mechanics*, 236, 91–103, 2016.

[5] Palabiyik, I., Olunloyo, B., Fryer, P. J., & Robbins, P. T., Flow regimes in the emptying of pipes filled with a Herschel–Bulkley fluid. *Chemical Engineering Research and Design*, 92(11), 2201–2212, 2014.

[6] Alba, K., Taghavi, S. M., and Frigaard, I. A., Miscible density-stable displacement flows in an inclined tube. *Physics of Fluids*, 24(12), 2012.

[7] Palabiyik, I., Lopez-Quiroga, E., Robbins, P. T., Goode, K. R., and Fryer, P. J., Removal of yield-stress fluids from pipework using water. *AIChE Journal*, 64(5), 1517–1527, 2018.

[8] Taghavi, S. M., Alba, K., Seon, T., Wielage-Burchard, K., Martinez, D. M., and Frigaard, I. A., Miscible displacement flows in near-horizontal ducts at low Atwood number. *Journal of Fluid Mechanics*, 696, 175–214, 2012.

[9] Taghavi, S. M., Alba, K., Moyers-Gonzalez, M., & Frigaard, I. A., Incomplete fluid–fluid displacement of yield stress fluids in near-horizontal pipes: Experiments and theory. *Journal of Non-Newtonian Fluid Mechanics*, 167-168, 59–74, 2012.

[10] Taghavi, S. M., Alba, K., and Frigaard, I. A., Buoyant miscible displacement flows at moderate viscosity ratios and low Atwood numbers in near-horizontal ducts. *Chemical Engineering Science*, 69(1), 404–418, 2012.

[11] Taghavi, S. M., A two-layer model for buoyant displacement flows in a channel with wall slip. *Journal of Fluid Mechanics*, 852, 602–640, 2018.

[12] Wiklund, J., Stading, M., and Trägårdh, C., Monitoring liquid displacement of model and industrial fluids in pipes by in-line ultrasonic rheometry. *Journal of Food Engineering*, 99(3), 330–337, 2010.

[13] Gabard, C., and Hulin, J.-P., Miscible displacement of non-Newtonian fluids in a vertical tube. *Eur Phys J E*, 11(3), 231–241, 2003.

[14] Zare, M., and Frigaard, I. A., Buoyancy effects on micro-annulus formation: density unstable Newtonian–Bingham fluid displacements in vertical channels. *Journal of Non-Newtonian Fluid Mechanics*, 260, 145–162, 2018.

[15] Zare, M., Roustaei, A., and Frigaard, I. A., Buoyancy effects on micro-annulus formation:

ISBN: 978-0-9984188-3-4; Published online www.heatexchanger-fouling.com

Density stable displacement of Newtonian–Bingham fluids. *Journal of Non-Newtonian Fluid Mechanics*, 247, 22–40, 2017.

[16] Hasnain, A., Segura, E., and Alba, K., Buoyant displacement flow of immiscible fluids in inclined pipes. *J Fluid Mech*, 824, 661–687, 2017.

[17] Alba, K., Taghavi, S. M., de Bruyn, John R., and Frigaard, I. A., Incomplete fluid–fluid displacement of yield-stress fluids. Part 2: Highly inclined pipes. Journal of Non-Newtonian Fluid Mechanics, 201, 80-93, 2013.

[18] Alba, K., and Frigaard, I. A., Dynamics of the removal of viscoplastic fluids from inclined pipes. *Journal of Non-Newtonian Fluid Mechanics*, 229, 43-58, 2016.

[19] Rothkopf, I., Interactions of fat migration and crystallization in filled dark chocolate products (Ph. D. thesis). Technische Universität München, Germany, 2023.

[20] Kumbár, V., Kouřilová, V., Dufková, R., Votava, J., and Hřivna, L., Rheological and Pipe Flow Properties of Chocolate Masses at Different Temperatures. *Foods*, 10(11), 2519, 2021.

[21] Liebmann, V., Heide, M., Köhler, H., Rüdiger, F., and Fröhlich, J., Improving flushing processes through targeted control of the temperature boundary conditions, *Proceedings in Applied Mathematics and Mechanics, Dresden*, Germany, vol. 23, 2023.

[22] Liebmann, V., Heide, M., Schoppmann, K., Köhler, H., Fröhlich, J., Rüdiger, F., Aspects of modelling the cleaning of a chocolate with yield stress in a pipe using CFD, *Fouling and Cleaning in Food Processing 2022 Proceedings*, 2022.

[23] ICA, Viscosity of cocoa and chocolate products. Analytical Method 46. CAOBISCO, Bruxelles, Belgium, 2000.

[24] Barbosa, C., Diogo, F., and Alves, M. R., Fitting mathematical models to describe the rheological behaviour of chocolate pastes. *AIP Conference Proceedings (AIP Conf. Proc.)*, 1738(1), 2016.

[25] Pitsillou, R., Georgiou, G. C., and Huilgol, R. R., On the use of the Lambert function in solving non-Newtonian flow problems. *Physics of Fluids*, 32(9), 2020.

ISBN: 978-0-9984188-3-4; Published online www.heatexchanger-fouling.com